Anomaly of $N=8$ shell closure in neutron-rich Be and B isotopes studied via delayed neutron emitting ^{14}Be β decay

N. Aoi* and K. Yoneda†
Department of Physics, University of Tokyo, 7-3-1 Hongo, Bunkyo, Tokyo 113-0033, Japan

E. Ideguchi, T. Kishida, T. Nakamura,‡ M. Notani,§ H. Sakurai,‖ T. Teranishi,§ Y. Watanabe, H. Wu,¶ and A. Yoshida
RIKEN (The Institute of Physical and Chemical Research), 2-1 Hirosawa, Wako, Saitama 351-0198, Japan

H. Miyatake** and Y. Yamamoto
Department of Physics, Osaka University, 1-1 Machikaneyama, Toyonaka, Osaka 560, Japan

H. Ogawa
Department of Applied Physics, Tokyo Institute of Technology, 2-12-1 Ookayama, Meguro, Tokyo 152-8551, Japan

S. S. Yamamoto†
Department of Physics, Sophia University, 7-1 Kioi-cho, Chiyoda-ku, Tokyo 102, Japan

M. Ishihara
Department of Physics, University of Tokyo, 7-3-1 Hongo, Bunkyo, Tokyo 113-0033, Japan
and RIKEN (The Institute of Physical and Chemical Research), 2-1 Hirosawa, Wako, Saitama 351-0198, Japan
(Received 21 February 2002; published 26 June 2002)

We investigated the β decay of the neutron drip line nucleus ^{14}Be by means of double and triple coincidence measurements of β rays, delayed neutrons, and γ rays. The decay sequences were established and new values of the half-life and branching ratios were obtained. The decay scheme obtained is characterized by a single dominant branch leading to a 1^+ state in ^{14}B with a branching ratio of $(91\pm9)\%$, which subsequently emits a delayed neutron with an energy of 288 ± 8 keV. The excitation energy and width of the 1^+ state were determined to be 1.28 ± 0.02 MeV and 49 ± 2 keV, respectively. The excitation energy and width of this level as well as the log *ft* value were treated in terms of a simple shell model and found to be strongly related to the $N=8$ shell gap quenching in^{13,14}B and ^{12}Be.

DOI: 10.1103/PhysRevC.66.014301 PACS number(s): 21.10.Hw, 23.20.Lv, 23.40.−s, 27.20.+n

I. INTRODUCTION

Neutron-rich nuclei far from the stability line have attracted much attention because of the expectation that the large excess of neutrons and loose binding of the valence neutrons may cause an interesting modification of their structure [1,2]. The ^{14}Be nucleus is such a neutron rich nucleus, located at the edge of the neutron drip line with a small two neutron separation energy of 1.34 ± 0.11 MeV [3]. Indeed, a neutron halo structure was indicated for this isotope by an enhanced interaction cross section [4,5], a narrow momentum distribution [6] observed in projectile breakup reactions, and the excitation energy and width of the IAS observed in the (p,n) reaction of ^{14}Be [7]. The halo structure is attributed to a large admixture of the $(2s_{1/2})_\nu^2$ configuration in the ground state wave function of the two valence neutrons [5,7–9].

For extremely neutron-rich nuclei around the neutron magic number $N=8$, a particular interest is directed to the phenomenon of shell gap quenching or the disappearance of magicity. This phenomenon was first discussed systematically for $N=7$ isotones by Talmi and Unna [10] in the study of the neutron single particle energies for the $(1p_{1/2})_\nu$ and $(2s_{1/2})_\nu$ orbitals, where the energy difference, $\Delta\epsilon = \epsilon(2s_{1/2})_\nu - \epsilon(1p_{1/2})_\nu$, between the two states may represent the shell gap between the p and sd shells. With increasing proton deficiency, $\Delta\epsilon$ decreases significantly, and the level order of the two states is even inverted in ^{11}Be [11]. Recent work on ^{10}Li [12–18] has revealed that this trend of the level inversion persists even in the $N=7$ Li isotope, ^{10}Li. The near degeneracy of the two single particle orbitals may strongly affect the wave functions of low lying states of the Be and Li isotopes around $N=8$ through an enhanced mixture of the configurations based on the $(2s_{1/2})_\nu$ and $(1p_{1/2})_\nu$

*Electronic address: aoi@phys.s.u-tokyo.ac.jp
†Present address: RIKEN (The Institute of Physical and Chemical Research), 2-1 Hirosawa, Wako, Saitama 351-0198, Japan.
‡Present address: Department of Physics, Tokyo Institute of Technology, 2-12-1 Ookayama, Meguro, Tokyo 152-8551, Japan.
§Present address: Center for Nuclear Study (CNS), University of Tokyo, Wako, Saitama 351-0198, Japan.
‖Present address: Department of Physics, University of Tokyo, 7-3-1 Hongo, Bunkyo, Tokyo 113-0033, Japan.
¶Present address: Institute of Modern Physics, Chinese Academy of Sciences, Lanzhou, 730000, China.
**Present address: High Energy Accelerator Research Organization (KEK), 1-1 Oho, Tsukuba Ibaraki 305-0801, Japan.

orbitals. For example, various observations indicate considerable mixing of $(2s_{1/2})^2_\nu$ and $(1p_{1/2})^2_\nu$ configurations for the ground states of ^{11}Li and ^{12}Be [19–23]. Shell gap quenching also causes lowering of the excitation energy of the $L=1$ mode, which has been observed in ^{11}Li [24,25] and ^{12}Be [26].

It is interesting to extend a systematic investigation to further clarify in what range of nuclei and to what extent the phenomenon of shell gap quenching is manifested. The present work has revealed several new features of this phenomenon through the β and neutron decay properties of nuclei around $N=8$.

β spectroscopy has long been utilized to investigate the structure of a variety of nuclei. In particular, for extremely neutron-rich nuclei, the scope of β spectroscopy has widened dramatically because of their unique β-decay properties. Since these nuclei have large Q_β's, excited states of the daughter nuclei over a wide range of excitation energy could be populated by β decays. Together with the small separation energies of the daughter nuclei, these β decays often lead to unbound states in the daughter nuclei, and therefore will be accompanied by particle emissions. In such a case particle emission follows the β decay. Indeed, delayed emissions of $n,2n,3n,4n,d,t,\alpha$, and ^{6}He have been observed in such β decays [27–31]. Among them, a one-neutron emission channel usually has the largest branching ratio. Thus the delayed neutron spectroscopy provides a useful means to investigate the structure of neutron-rich nuclei.

The case of the ^{14}Be β decay affords a typical example: Q_β of ^{14}Be is as large as 16.22 ± 0.11 MeV [32], and consequently the half-life is as short as $t_{1/2}=4.35\pm0.17$ ms [31]. The delayed neutron emission probabilities have been investigated by two groups. Dufour *et al.* [31] reported $P_{0n}=(14\pm3)\%$, $P_{1n}=(81\pm4)\%$, and $P_{2n}=(5\pm2)\%$ and Bergmann *et al.* [33] reported $P_{0n}<4\%$, $P_{1n}>96\%$, and $P_{2n}+3P_{3n}<1.6\%$ (1σ), where P_{in} denotes the probability of emitting i neutron(s). Though the results do not agree with each other, both experiments exhibit fairly large probabilities of neutron emissions.

In a recent work [34], an attempt was made to measure the energy spectrum of the delayed neutrons, and two weak neutron peaks were observed at 3.52 ± 0.07 MeV and 3.02 ± 0.03 MeV with the branching ratios of $(0.11\pm0.02\pm0.04)\%$ and $(0.30\pm0.03\pm0.05)\%$, respectively. In a more recent work at RIKEN [35], where the measurement of the neutron spectrum was extended to lower energies, a single dominant peak was found at a very low energy of 287 ± 3 keV with a branching ratio of $43-100\,\%$. Such a large branching ratio can only be caused by a Gamow-Teller (GT) transition. This leads to 1^+ assignment to the daughter state in ^{14}B, since the parent state of ^{14}Be ground state has spin/parity 0^+. If the 1^+ state is located at a low excitation energy, it represents an intruder state of non-normal parity, which would occur due to possible shell gap quenching in $N=9$ isotone, ^{14}B. Thus, much refined data on this branch would be important for exploring the phenomenon of reduced magicity. Experimentally, a large uncertainty still remained in the magnitude of the branching ratio due to the difficulty in detecting the low energy neutron peak mentioned above. There also remained an ambiguity of the location of the ^{14}B (1^+) state, since the decay sequence could not be uniquely identified for the lack of coincidence measurements of delayed neutrons with β rays and γ rays. These properties are essential for a close investigation of the nuclear structure of ^{14}Be and its daughter nuclei.

In the present work, as briefly reported in Refs. [36,37], we aimed at an unambiguous determination of the decay scheme of ^{14}Be in order to obtain a better picture of the nuclear structures of neutron-rich boron and beryllium isotopes. For this purpose we incorporated upgraded detectors for neutrons and γ rays as well as for β rays. In particular, much care was taken to increase the detection efficiencies so that even a β-n-γ triple coincidence analysis would be possible. This capability proved to be powerful in uniquely determining the decay sequences. An effort was also made to improve the low energy performance of the neutron detectors, which was essential for obtaining accurate data on the neutron peak near 287 keV.

In the following, we first describe the experimental setup and procedure in Sec. II. In Sec. III, the experimental results are described, where the observed half-life of ^{14}Be β decay, the width, and energy of the strong neutron peak and the branching ratio of this neutron emission are presented. Based on the new results, we determine the decay sequence from the triple coincidence analysis and establish the decay scheme of ^{14}Be in Sec. IV. Using these results we discuss in Sec. V three different subjects related to the phenomenon of shell gap quenching. First, the systematic behavior of $\Delta\epsilon$ is discussed for $N=9$ isotones by incorporating the result of the ^{14}B (1^+) excited state, whose location was established in the present work. It is found that the behavior of $\Delta\epsilon$ for $N=9$ as a function of Z is almost the same as that for $N=7$ isotones. Second, the wave function of the ^{13}B ground state in terms of shell model configurations is discussed based on the width of the strong neutron peak, which represents the transition probability between the ^{14}B (1^+) state and ^{13}B ground state. Considerable mixing of the $(2s_{1/2})^2_\nu$ and $(1p_{1/2})^2_\nu$ configurations is indicated. Finally, the log ft value obtained is compared to that of the analogous β branch of another $N=8$ nucleus, ^{12}Be. A clear effect of shell gap quenching is again observed in the ground state of ^{12}Be.

II. EXPERIMENTAL SETUP AND PROCEDURE

The measurement of the ^{14}Be β decay was performed at the RIKEN Accelerator Research Facility. The β decays of ^{17}N and ^{13}B were also observed to calibrate the detectors. The radioactive beams of ^{14}Be,^{17}N, and^{13}B, were produced using the projectile-fragment separator, RIPS [38], by ^{18}O induced projectile fragmentation reactions on a 1.48 g/cm^2 thick Be target at 100A MeV. The secondary ^{14}Be beam had an intensity of about 300 particles per second and an isotope purity of 86%. The impurity is mostly due to tritons that hardly disturbed the β-decay measurements because of their long half-life.

The radioactive ions were transported to the final focal point of RIPS and were implanted in a stopper of a 1-mm-

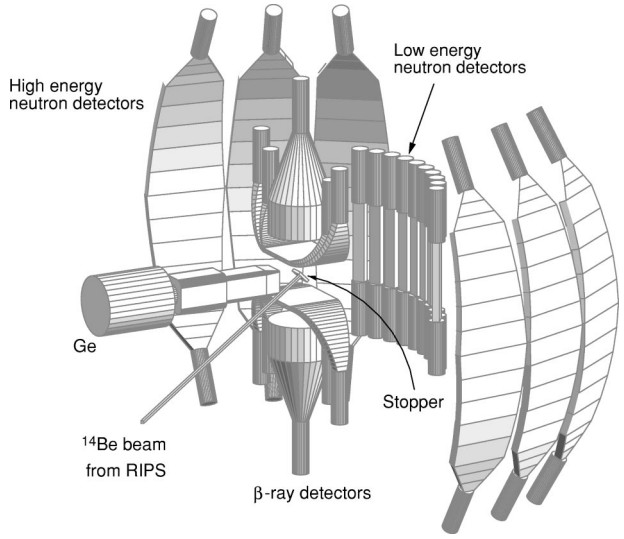

FIG. 1. Experimental setup for the β-decay measurement of ^{14}Be.

thick Si detector. A rotatable aluminum plate was placed upstream of the stopper to reduce the energy of the ions. The angle of the plate was adjusted so as to stop the ions in the middle of the stopper in the beam direction. For the deduction of the implantation depth of the ions in the stopper, the energy signals of the stopper and plastic scintillators (1 mm thick) located at the front and the back of the stopper were used.

The beam was pulsed to facilitate the measurement of half-life spectra and to obtain better signal-to-noise ratios. The durations of beam-on and -off periods were chosen to be 15 ms and 40 ms, respectively, to match the half-lives of ^{14}Be (4.35 ms [39]) and its daughters, ^{14}B (13.8 ms [39]),^{13}B (17.36 ms [39]), and ^{12}B (20.20 ms [40]).

The delayed γ rays and neutrons as well as the β rays were measured using the array of detectors located around the stopper as schematically shown in Fig. 1. In the following, the experimental setup and performance of the detectors are described in more detail. The scheme of the data acquisition procedure is also described.

A. β-ray detectors

β rays from the stopped nuclei were detected by two sets of ΔE-ΔE-E plastic scintillator telescopes placed above and below the stopper. Each ΔE counter had a size of $200\times200\times2$ mm^3. The ΔE detectors located closest to the stopper were placed 8.3 cm above and below the stopper, covering 42% of the solid angle. The intrinsic detection efficiency was found from the Monte Carlo simulation to be nearly 100% for β rays with energies above 2.5 MeV. Each ΔE detector had a photomultiplier tube at each end and the logical AND of two signals defined the detection of a β ray. The average of the timing signals from the two photomultiplier tubes provided the detection time. The two ΔE counters in each β-ray telescope enabled a ΔE-ΔE coincidence to suppress the counting rate due to a possible high rate γ-ray background. It turns out, however, that the counting rate due to this background was sufficiently low (of the order of 10 cps). Therefore, only the signals from the first layer ΔE counters closest to the stopper were used as the trigger. Each E counter had a cylindrical shape with a diameter of 240 mm and a height of 130 mm. The large thickness of the detector allowed the measurement of a β-ray energy up to about 30 MeV.

B. Neutron detectors

For the detection of the delayed neutrons, plastic scintillators were utilized. The neutron energy was determined from its time of flight (TOF), which was derived from the time difference between the β ray and neutron signals. In order to cover a wide energy range of neutrons, two different sets of plastic scintillators were used: one for low energies below about 1 MeV and the other for high energies above 1 MeV.

The low energy setup consisted of nine short plastic scintillators with a size of $300\times45\times25$ mm^3. They were located about 50 cm away from the stopper and covered a solid angle of 3.5% of 4π sr. Two photomultiplier tubes attached at both ends of each scintillator read out light outputs and the average timing of these two signals was used to define the neutron detection timing. Special care was taken to facilitate the detection of low energy neutrons around 287 keV. The main difficulty in detecting such low energy neutrons comes from their weak scintillation. The short length of the plastic scintillators improved the light collection efficiency, and an energy threshold as low as 5 keV electron equivalent (keVee) was achieved. This enabled the low energy neutron measurement with a high and reliable efficiency.

The parameters for the neutron detectors, the flight length, TOF resolution, and detection efficiency were calibrated using the delayed neutron spectrum observed in the ^{17}N β decay, which is known to be accompanied by delayed neutron emissions with the energies of 382.8 ± 0.9 keV, 1170.9 ± 0.8 keV, and 1700.3 ± 1.7 keV with the respective branching ratios of (38.0 ± 1.3)%, (50.1 ± 1.3)%, and (6.9 ± 0.5)% [41]. The TOF resolution (σ_t) was evaluated assuming a functional form of σ_t as a function of TOF (t) to be

$$\sigma_t^2=\sigma_0^2+\left(\frac{\sigma_L}{L}t\right)^2,$$

where σ_0 is due to the intrinsic timing resolutions of the β-ray and neutron detectors, and σ_L represents the finite spread of the flight length (L) due to the beam spot spread and the thicknesses of the neutron detectors. The values of σ_0 and σ_L were then found to be 3.94 ± 0.04 ns and 3.1 ± 0.1 cm, respectively, leading to the energy resolution of 20 keV for the 287-keV neutrons of interest.

The detection efficiency for the 383-keV neutron peak from ^{17}N was deduced to be (70 ± 7)%. In order to extrapolate the detection efficiency from 383 keV down to 287 keV, the relative efficiencies for different energies were measured in a separate experiment using neutron beams produced by the ^{7}Li$(p,n)^7$Be reaction. The Pelletron accelerator at the Research Laboratory for Nuclear Reactors (RLNR) at the To-

kyo Institute of Technology was used for this purpose. It was found that the efficiency in the energy range between 200 keV and 400 keV was constant within the experimental uncertainty. This was consistent with the expectation from the low energy threshold used (5 keVee), which is far below the neutron energies of interest. On this basis, the efficiency for the 287-keV neutrons was taken to be the same as that for the 383-keV neutron.

The other neutron detector, the high energy neutron detector array [42], was placed about 1.5 m away from the stopper. It consisted of six identical plastic scintillators, each of which had a volume of $160\times40\times2$ cm^3 and was bent to have a 1.5-m radius of curvature so that neutrons emitted at the stopper had a uniform flight length. The overall solid angle was 10% of 4π sr. This detector had a long flight length, which provided a good energy resolution for high energy neutrons. The calibration with the ^{17}N beam yielded the flight length of 150.8 ± 0.4 cm, the energy resolution of 50 keV at 2 MeV, and the detection efficiency of 20% at 2 MeV.

C. γ-ray detectors

γ rays were detected by a Clover Ge detector [43] placed at 14.9 cm from the stopper. The detection efficiency was calibrated using a ^{152}Eu standard source in the energy range from 211 keV to 2125 keV. The known delayed γ rays from^{13}B (3685 keV) and ^{17}N (871 keV) were also used for the energy and efficiency calibration.

D. Data acquisition system and triggers

The data acquisition system was triggered by a signal given as a logical OR of the first layer ΔE counters of the β-ray telescopes, one above and the other below the stopper. The signals from all the other counters, i.e., the β-ray telescopes and neutron and γ-ray detectors, were recorded simultaneously. The events with significant signals from the neutron and/or γ-ray detectors were selected off-line for the analysis of β-n and β-γ double coincidence and β-n-γ triple coincidence data.

To obtain the decay curves for the above three coincidence data, the time of each event measured from the start of the beam-on period was also recorded. Since the shape of the decay curves could be distorted by the rate dependence of the dead time in the data acquisition system, random pulses were mixed with the β triggers, so that the dead time spectrum was deduced and was used to correct for the distortion of the decay curves.

III. DATA ANALYSIS AND RESULTS

In this section we describe the procedures and results of the data analysis with emphasis on the decay curves and energy spectra of neutrons and γ rays. The decay spectrum obtained without coincidence was used to determine the number of observed β decay of ^{14}Be. For the determination of the half-life of ^{14}Be, the decay curve from β-n data was used.

The neutron and γ-ray energy spectra to be analyzed were both taken in coincidence with the β-trigger signals. The spectra are fairly simple, being dominated by few peaks. The neutron TOF spectrum (Fig. 2) shows a single large peak around 288 keV, for which the energy, width, and branching ratio were obtained. There were no other clear peaks observed in the neutron spectrum except for a very weak peak near 3.52 MeV. Similarly, the γ-ray spectrum (Fig. 3) involves only two significant peaks relevant to the β decay of ^{14}Be and its daughter nucleus: one at 3685 ± 1 keV and the other at 3536 ± 2 keV. These γ rays are ascribed to the transitions in^{13}C and ^{13}B, respectively. The former is due to the β decay of the daughter nucleus ^{13}B, while the latter is the γ decay from the state in^{13}B reached by the delayed neutron

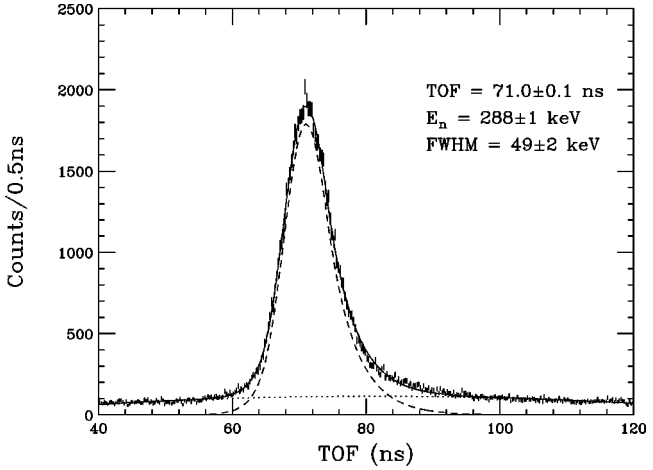

FIG. 2. TOF spectrum of neutrons emitted in the decay of ^{14}Be obtained with the low energy detectors. A significant neutron peak is seen at 71 ns, which corresponds to 288 keV in neutron energy. The solid line is a fit to the observed spectrum, which contains a hyper-Gaussian peak (dashed line) and a parabolic-shaped background (dotted line).

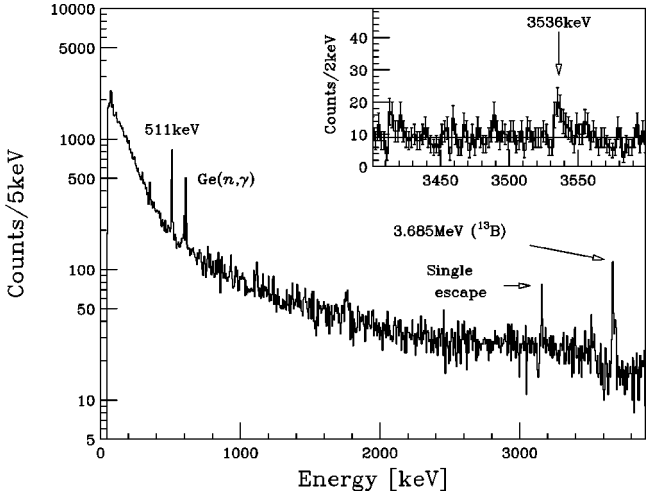

FIG. 3. Energy spectrum of γ rays obtained with the Ge detectors. The significant peak at 3.685 MeV is assigned to the delayed γ ray of the daughter nucleus ^{13}B. The inset shows the spectrum around the 3500-keV region. The weak line at 3536 keV corresponds to the decay from the first excited state to the ground state of ^{13}B.

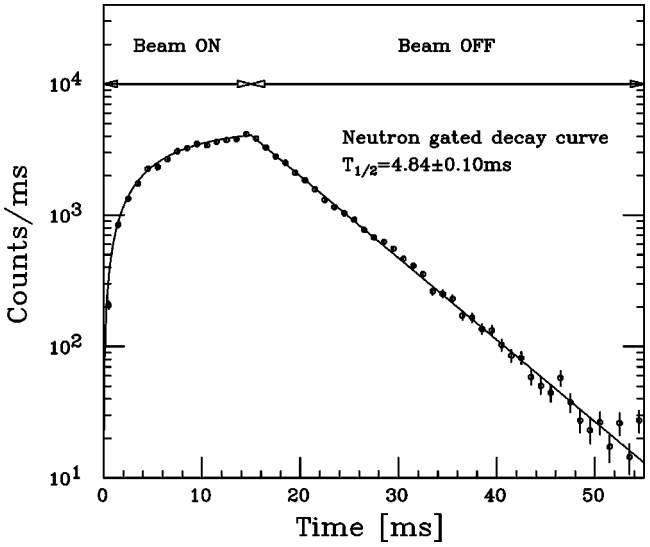

FIG. 4. Decay curve obtained in coincidence with the 288-keV neutron peak. The ^{14}Be beam was on during the first 15 ms, and was off during the subsequent 40 ms. The solid line shows a fit to a single decay plus a constant background.

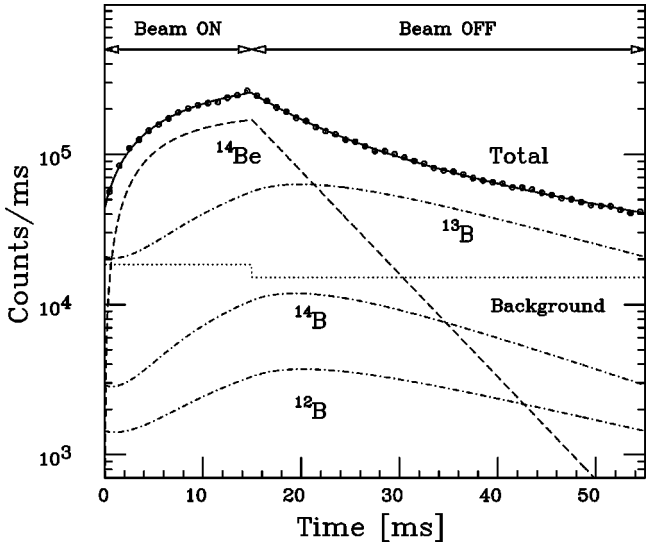

FIG. 5. Raw decay curve of ^{14}Be. The solid line indicates a fit to a function that includes the decay of ^{14}Be (dashed line), those of its daughter nuclei, ^{14,13,12}B (dot-dashed lines), and a background (dotted line).

emission of ^{14}Be. In the following, the details of the analysis are presented for these spectra. Coincidence relations will be mainly discussed in the following section in connection with the proposed decay scheme.

A. Decay curves

The decay curve obtained in coincidence with the 288-keV neutrons was used for the determination of the half-life of ^{14}Be taking advantage of being almost free from the contamination from the decay of the daughter nuclei, ^{14}B, ^{13}B, and ^{12}B. In fact, the coincident decay spectrum was well fitted to a single decay component plus a constant background as shown in Fig. 4 (solid line). From the fit, a half-life of 4.84 ± 0.10 ms was obtained with a reduced χ^2 of 1.18. The newly determined half-life is slightly longer than those of the previous works, i.e., 4.35 ± 0.17 ms [31] and 4.29 ± 0.16 ms [35]. The reason of these discrepancies is not yet clear.

The count N_β defines the number of observed β decays of ^{14}Be and provides the normalization factor to determine the ratios of the β-decay branches. It was obtained from the decay curve without coincidence with γ rays or neutrons. This decay curve involved contributions from ^{14}Be and its three daughters, ^{14}B, ^{13}B, and ^{12}B. The decomposition of the different components required a careful analysis of the spectrum, since the three daughters have similar half-lives. The raw decay curve was fitted to a function consisting of five components: the β rays from ^{14}Be and its three daughters (^{14}B, ^{13}B, and ^{12}B) and constant backgrounds (Fig. 5). In the fit, the half-life of ^{14}Be was fixed at the new value obtained from the present data (4.84 ms) while those of the daughter nuclei, ^{14}B, ^{13}B, and ^{12}B were fixed at the known values of 13.8 ms, 17.36 ms [39], and 20.20 ms [40], respectively. The relative β-ray intensities of the decays from the different daughters, $^{14-i}$B ($i=0,1,2$), were fixed at the multineutron emission probabilities P_{in} obtained in Ref. [31]. The background levels for the beam-on and -off periods were separately given, since the background level might increase during the beam-on period. The free parameters of the fit were, thus, N_β and the magnitudes of the two backgrounds.

The value of N_β was then obtained to be $(3.28\pm0.02)\times10^6$ counts, where the quoted error is the statistical error. An additional error due to the uncertainties of the values used for the ^{14}Be half-life and P_{in} was estimated by changing these parameters within the ranges of their possible uncertainties. For instance, fits with the ^{14}Be half-lives obtained in Refs. [31,35] were performed, but the resulting values of N_β all agreed with one another within the fitting error. Fits with several sets of P_{in} values including the newly obtained ones to be described later in this paper were also performed. The changes in P_{in} values hardly affected the decay spectrum so long as their sum was fixed at 100%, since the half-lives of three daughters are fairly close to one another. Therefore, the systematic error of 1% was assigned to N_β. This error is negligible in the deduction of the branching ratio because it is much less than the experimental uncertainty in the number of neutrons N_n from the neutron emissions.

B. Neutron TOF spectra

The shape of the strong peak at around 70 ns in the TOF spectrum was fitted to determine its central energy, width, and yield (N_n) as shown in Fig. 2 (solid line). The peak shape is not symmetric like those found in the neutron spectra observed in the β decays of several other nuclei [35,44]. Although the origin of this asymmetry was not fully understood, the neutron peak was fitted to a hyper-Gaussian function as used in Ref. [35]. This function consisted of four components: two exponentials for the tails on both sides of the peak and two Gaussians for the left and right sides of the

peak. Even though the slopes and widths of the four curves were separately given, they were constrained to connect smoothly. The background is assumed to have a parabolic shape. The result of the χ^2 fit is shown in Fig. 2, where dashed and dotted lines represent the peak and background shape, respectively, and solid line shows their sum. The central peak position obtained was 71.0 ± 0.1 ns, which corresponds to 288 ± 1 keV in neutron energy. The quoted error includes the uncertainty in the flight length as well as the statistical error. The full width at half maximum was obtained to be 8.3 ± 0.1 ns, which corresponds to 49 ± 2 keV, after correcting for the detector timing resolution of 5.7 ± 0.2 ns. These results are fairly consistent with those from the previous measurement [35]. The total yield N_n of the neutron peak was obtained from the same fit to be $(8.92 \pm 0.04) \times 10^4$ counts. In order to estimate the uncertainty due to the choice of the background shape, a fit with a constant level background was also performed. It was found that the variation in the N_n value was much less than the uncertainty due to the neutron detection efficiency.

Using the obtained N_n value together with N_β and the neutron detection efficiency of $(70 \pm 7)\%$, the branching ratio for the 288-keV neutron peak was deduced to be $91 \pm 9\%$. This value agrees with that obtained in the previous experiment $(38-100\%)$ [35] while the accuracy has increased significantly.

We also studied the weak neutron peaks at 3.52 MeV and 3.02 MeV as reported in Ref. [34]. The high energy detector was used for this purpose. In the neutron TOF spectrum, a neutron peak was observed at 3.51 ± 0.06 MeV with a branching ratio of $(0.23 \pm 0.13)\%$, in agreement with the values of 3.52 ± 0.07 MeV and $(0.11 \pm 0.02 \pm 0.04)\%$ obtained in Ref. [34]. However, we studied the possibility that this neutron peak is due to the delayed neutron emission in the β decay of ^{13}B, for which the energy and branching ratio ($I_n^{(3.55)}$) are known to be 3.55 ± 0.10 MeV and $(0.16 \pm 0.03)\%$ [45], respectively. Since ^{13}B is produced as the daughter of ^{14}Be in the one-neutron emission process, the branching ratio of this neutron peak with respect to the ^{14}Be decay should be the product, $P_{1n} \times I_n^{(3.55)}$. Using the P_{1n} value of $(94 \pm 5)\%$ to be obtained in the following section, $P_{1n} \times I_n^{(3.55)}$ is calculated to be $(0.20 \pm 0.04)\%$, which is indeed consistent with the observed neutron intensity. An analysis of the decay curve or γ spectrum in coincidence with this peak, which might be helpful to confirm the above possibility, was not performed because of the low statistics.

As for the other possible neutron peak at 3.02 MeV [34], no significant peak was observed there. However, the existence of this peak cannot be totally ruled out because of the presence of a continuous background with a magnitude comparable to the strength of 3.02-MeV peak reported in Ref. [34].

C. γ-ray energy spectra

In the γ-ray spectrum (Fig. 3), two lines with significant intensities appeared at 3536 ± 2 keV and 3685 ± 1 keV. The 3536-keV line is ascribed to the γ transition from the first excited state to the ground state of ^{13}B. The branching ratio of the γ transition was found to be $(0.9 \pm 0.3)\%$, which is consistent with the previous result of about 0.6% [34]. Its intensity is likely to account for almost the whole population fed by the delayed neutrons feeding the excited states of ^{13}B. The small branching ratio of this line indicates that the 288-keV neutron peak dominating the $1n$ emission channel should directly feed the ground state of ^{13}B.

The 3685-keV line is ascribed to the transition from the second excited state of ^{13}C, which is reached by the β decay of ^{13}B. The intensity of this line provides a measure of the yield of ^{13}B in the decay of ^{14}Be, i.e., P_{1n}, which is further discussed in the following section.

IV. DECAY SCHEME OF ^{14}Be

In this section the decay scheme of ^{14}Be is discussed using the results obtained in Sec. III together with the results of the triple coincidence data (see Fig. 6). The spin/parity assignment to the ^{14}B state involved in the observed neutron transition is made on the basis of the $\log ft$ value. Furthermore, new values of the half-life and P_{in} are presented.

The decay scheme involves a fairly small number of branches. The major branch is associated with the strong neutron peak at 288 keV shown in Fig. 2. The 288-keV neutron transition is ascribed to the $1n$ channel, because no other neutron peak with comparable strength was observed in the TOF spectrum. To confirm this, an analysis of the β-n-n coincidence data was made, and no significant neutron peak was seen in coincidence with the 288-keV neutron peak. Therefore, it was concluded that the neutron is emitted in the transition from the unbound state in ^{14}B to the bound state in ^{13}B. To identify the final state of the neutron transition, the γ-ray spectrum was analyzed by requiring an additional coincidence with the 288-keV neutron peak (Fig. 7). If the neutron transition goes to an excited state, a deexcitation γ ray from the excited state should appear in this β-n-coincident γ-ray spectrum. For example, if the neutron transition is to the first excited state of ^{13}B ($E_x = 3.535$ MeV), a photoelectric γ-ray peak with more than 75 events should be seen in the spectrum (dotted line). In the obtained spectrum, however, no significant peak is observed with very low background level (<0.1 counts per keV). This fact strongly indicates that the neutron transition goes directly to the ground state of ^{13}B. The energy difference between the initial and final states of the neutron transition is obtained to be 310 keV from the central energy of the 288-keV neutron peak after correcting for the recoil of ^{13}B. Thus the neutron emitting state was determined to be located at 1.28 ± 0.02 MeV in ^{14}B as shown in Fig. 6, where the excitation energy is given by the sum of the known neutron separation energy of ^{14}B ($S_n = 970 \pm 20$ keV [3]) and the neutron transition energy. The error is mainly associated with the uncertainty in S_n.

Using the result of the partial half-life and the decay energy, we obtained a $\log ft$ value of 3.68 ± 0.05 for the β branch to the 1.28-MeV level, which is very small compared to those for most of the β decays of the neighboring nuclei. This value turns out to be one of the smallest values among the known β^- decays. The small $\log ft$ value indicates that

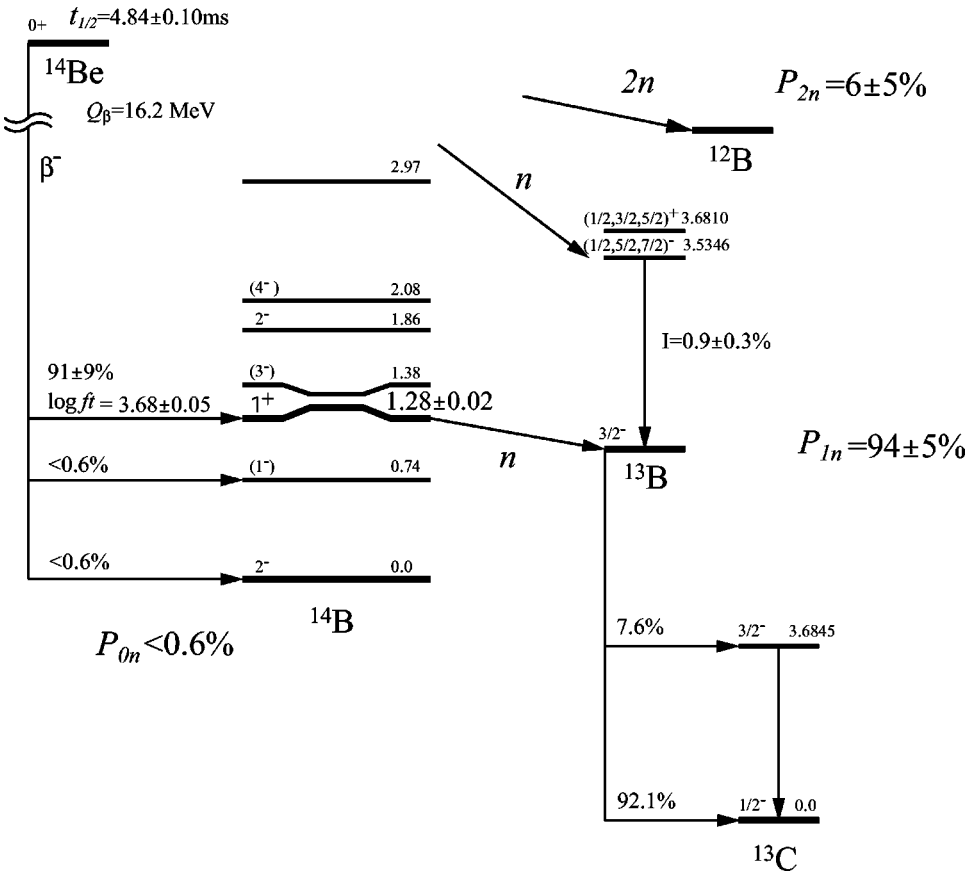

FIG. 6. Decay scheme of ^{14}Be deduced from neutron and γ-ray spectra. The excitation energies are indicated in MeV. The excited state at 1.28 MeV in ^{14}B is identified for the first time in this work.

the decay is due to a GT transition. The possibility of a Fermi transition may be excluded, since the Fermi transition strength is usually concentrated on the isobaric analog state of ^{14}Be. The selection rule for the GT transition from the 0^+ parent state uniquely determines the spin and parity of the final state to be 1^+.

The i-neutron emission probabilities, P_{in} $(i=0,1,2)$, were determined from the delayed γ-ray intensities of the daughter nuclei. After the i-neutron emission, the whole population eventually feeds the ground state of $^{14-i}$B, by ignoring weak branches accompanying emissions of both neutrons and charged particles such as d, t, and α. The daughter nuclei, ^{14}B, ^{13}B, and ^{12}B, are β unstable, and their decay schemes are well known. Thus the P_{in} values can be determined by measuring delayed γ rays in the β decays of these nuclei.

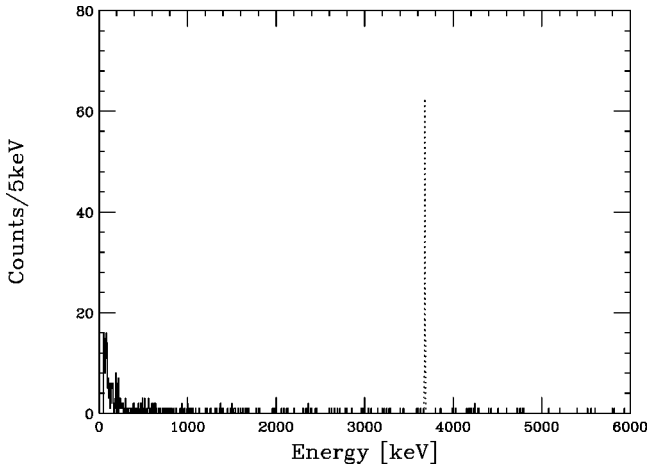

FIG. 7. The γ-ray spectrum in coincidence with the 288-keV neutron peak. The dotted line indicates the photopeak, which is expected in the case that the neutron emission leads to the first excited state of ^{13}B. The absence of any γ-ray peak with a comparable intensity proves that the neutron emission leads to the ground state of ^{13}B.

For the determination of P_{1n} we used the 3685-keV γ-ray transition in ^{13}C, which is emitted following the β decay of ^{13}B with the known branching ratio of $7.6\pm0.8\,\%$ [39]. The population of ^{13}B, i.e., P_{1n}, is then obtained from the γ-ray counts by incorporating the product of the γ-ray detection efficiency and this branching ratio. Instead of determining the two values separately, their product was directly obtained in a separate run, where a ^{13}B beam was produced by RIPS, and the numbers of ^{13}B ions and the 3685-keV γ rays were counted from the decay curve and the β-γ coincidence spectrum as done for ^{14}Be in Sec. III. By this method with little background, the uncertainty was considerably reduced. The P_{1n} value was then determined to be $(94\pm5)\%$. This value is compatible with the branching ratio of the 288-keV neutron peak $[(91\pm9)\%]$ within the experimental uncertainty. This closeness indicates that the $1n$-emission channel is almost exhausted by the 288-keV neutron transition.

The probability of the decay without neutron emission, i.e., P_{0n}, represents the sum of the intensities of the branches to the bound states in ^{14}B. Two bound states are known for ^{14}B [39]; the ground state and the first excited state ($E_x=740$ keV). To determine P_{0n}, delayed γ rays of ^{14}B

were examined. The β-decay scheme of ^{14}B involves the emission of the delayed γ ray of the energy of 6.09 MeV with the large branching ratio of $(81\pm9)\%$ [39]. In the observed spectrum, however, this line was not clearly identified, and only an upper bound of P_{0n} was determined to be 0.6% at a 90% confidence level. The γ ray emitted in the transition from the first excited state to the ground state was not seen either. This fact is consistent with the obtained upper bound of the P_{0n}. A lower limit of the log *ft* value was then deduced to be 5.8 or 5.7 when the final state was assumed to be either the ground or first excited states.

As for the $2n$ emission channel leading to ^{12}B, a significant probability is expected from the earlier result ($P_{2n}=5\%$ [31]). In contrast to the cases of P_{0n} and P_{1n}, the determination of P_{2n} was difficult, because the β decay of ^{12}B does not involve any delayed γ rays with significant branching ratios. Thus, the P_{2n} value was indirectly deduced to be $(6\pm5)\%$ assuming the relation, $P_{0n}+P_{1n}+P_{2n}=1$.

The obtained neutron emission probabilities [$P_{0n}<0.6\%$, $P_{1n}=(94\pm5)\%$, and $P_{2n}=(6\pm5)\%$] agree well with the result of Bergmann *et al.* ($P_{0n}<4\%$, $P_{1n}>96\%$, and $P_{2n}+3P_{3n}<1.6\%$ (1σ) [33]) but not quite well with the result of Dufour *et al.* [$P_{0n}=(14\pm3)\%$, $P_{1n}=(81\pm4)\%$, and $P_{2n}=(5\pm2)\%$ [31]]. In particular, the P_{0n} value is related to the spin/parity assignments for the ground and first excited states of ^{14}Be. The small P_{0n} value observed in this work indicates that the transitions to these states are due to first forbidden transitions, in agreement with the presently adopted assignments of 2^- and (1^-). On the other hand, the larger value obtained in Ref. [31] rather indicates positive parity assignments to these states.

V. DISCUSSION

In this section we discuss three different subjects related to the phenomenon of shell gap quenching based on the results obtained in the present experiment. First, in Sec. V A the systematic behavior of $\Delta\epsilon=\epsilon(2s_{1/2})_\nu-\epsilon(1p_{1/2})_\nu$ is discussed for $N=9$ isotones by incorporating the result of the ^{14}B (1^+) excited state. It is found that the behavior of $\Delta\epsilon$ for $N=9$ isotones as a function of Z is very similar to that for $N=7$. In Secs. V B and V C, the ground state wave functions of the two $N=8$ nuclei, ^{13}B and ^{12}Be are discussed in terms of shell model configurations. For the case of ^{13}B, the result of the neutron decay width of the ^{14}B(1^+) state is used and a strong indication that the configurations involving the $(2s_{1/2})_\nu$ and $(1p_{1/2})_\nu$ orbitals are considerably mixed is provided. For ^{12}Be, the log *ft* values of the corresponding β transitions from ^{12}Be and ^{14}Be are compared. Again a clear effect of shell gap quenching is indicated. In the following discussions, we take a simple shell model description, where we assume as a core a hypothetical ^{12}Be nucleus with the configuration of $|0\rangle=|(1s_{1/2})_\pi^2(1p_{3/2})_\pi^2(1s_{1/2})_\nu^2(1p_{3/2})_\nu^4\times(1p_{1/2})_\nu^2\rangle$ and configurations of neighboring nuclei are given with respect to this configuration.

A. Reduction of the shell gap energy in ^{14}B deduced from the excitation energy of ^{14}B (1^+) state

A notable feature of the newly identified 1^+ state at 1.28 MeV in ^{14}B is that it is located at a very low excitation energy although it has a positive (non-normal) parity. In normal nuclei around $N=8$, a non-normal parity state rarely appears at such a low excitation energy, since the $1p$ and $2s$-$1d$ shells are well separated. One of the exceptional cases is found in ^{11}Be, where spin/parity of $1/2^+$ is manifested in the ground state. In this regard Talmi and Unna systematically studied the energy difference $\Delta\epsilon$ between the $1p_{1/2}$ and $2s_{1/2}$ single-particle levels [10]. For neutron-rich $N=7$ isotones, they found that $\Delta\epsilon$ decreases rapidly with decreasing atomic number Z (dashed lines in Fig. 8): $\Delta\epsilon$ is 3.09 MeV in ^{13}C, while ^{12}B has a smaller $\Delta\epsilon$ value, 1.44 MeV. Finally, in ^{11}Be, $\Delta\epsilon$ has a negative value of -0.32 keV, indicating that the $1p_{1/2}$ and $2s_{1/2}$ single-particle states are inverted. An intriguing question of whether such a behavior persists in the isotones of different N will be discussed below.

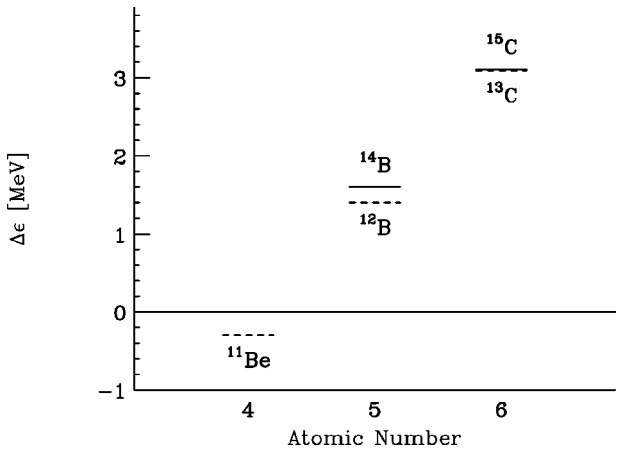

FIG. 8. Energy difference $\Delta\epsilon$ between $2s_{1/2}$ and $1p_{1/2}$ orbitals for the nuclei with neutron number 7 (dashed lines) and 9 (solid lines) as a function of atomic number.

In the following, we study $\Delta\epsilon$ for $N=9$ isotones by incorporating the present result of the ^{14}B (1^+) state. To extract the single-particle energies for ^{14}B, the procedure of Ref. [10] was followed. Since ^{14}B is an odd-odd nucleus, the single-particle energies for $(2s_{1/2})_\nu$ and $(1p_{1/2})_\nu$ are to be determined from the centers of mass of the lowest $(2^-, 1^-)$ and $(1^+, 2^+)$ doublets, respectively. The $(2^-, 1^-)$ doublet is supposed to be due to the $|(1p_{3/2})_\pi(2s_{1/2})_\nu\rangle$ configuration, while the $(1^+, 2^+)$ doublet is due to the $|(1p_{3/2})_\pi(2s_{1/2})_\nu^2(1p_{1/2})_\nu^{-1}\rangle$ configuration. We assume that the ground state and the first excited state ($E_x=740$ keV) form the $(2^-, 1^-)$ doublet. Then the center of mass is found to be 0.3 MeV. We then assume that the observed 1.28-MeV 1^+ state is a member of the $(1^+, 2^+)$ doublet. Since no 2^+ state has been found in ^{14}B so far, its excitation energy was estimated assuming the energy split between the 1^+ and 2^+ states to be the same as that for ^{12}B. The center of mass of the $(1^+, 2^+)$ doublet in ^{14}B therefore was estimated to be 1.9 MeV.

Using these centers of mass and assuming the same pairing energy for the $(1p_{1/2})_\nu$ and $(2s_{1/2})_\nu$ orbitals, the $\Delta\epsilon$ value of 1.6 MeV in ^{14}B was obtained. This value of $\Delta\epsilon$ is plotted in Fig. 8 (solid line) together with that for the adjacent $N=9$ nucleus, ^{15}C, which was obtained to be 3.1 MeV from the energies of the lowest $1/2^-$ and $1/2^+$ states. It is

interesting to note that the behavior of $\Delta\epsilon$ with Z is very similar to that for the $N=7$ isotones, and that the value of $\Delta\epsilon$ is considerably reduced at $Z=5$ as compared with that at $Z=6$. This finding is consistent with the enhanced magnetic moment of ^{14}B [46], which can be explained by lowering the $2s_{1/2}$ orbital with respect to the $1d_{5/2}$ orbital in ^{14}B.

B. Reduction of the shell gap energy in ^{13}B deduced from the width of ^{14}B (1^+) state

In general, the width of a neutron emitting state is controlled by the overlap of the initial and final state wave functions and the penetrability of the emitting neutron. In the present case, the emission of the 288-keV neutron is ascribed to the transition from the ^{14}B state (1^+) to the ground state of ^{13}B $(3/2^-)$. Thus the observed width can be used to pin down the structure of the ground state of ^{13}B. Considering the spin/parity of the initial and final states, the decay should occur primarily by p-wave neutron emission.

To allow a p-wave emission, the wave function of the final state should involve a configuration with one neutron hole at the p orbital with respect to that of the ^{14}B initial state. Considering that the major configuration of this ^{14}B (1^+) state is expressed as $|(1p_{3/2})^1_\pi(1p_{1/2})^{-1}_\nu(2s_{1/2})^2_\nu\rangle$, the $3p$-$2h$ configuration of $|(1p_{3/2})^1_\pi(1p_{1/2})^{-2}_\nu(2s_{1/2})^2_\nu\rangle$ is required for the final state wave function to allow the p-wave neutron emission. On the other hand, the wave function of the ^{13}B ground state is supposed to be mainly composed of the $|(1p_{3/2})^1_\pi\rangle$ configuration when the shell gap is considerable at $N=8$. This configuration is, however, forbidden for a p-wave neutron emission from the ^{14}Be (1^+) state. To resolve this inconsistency, the following configuration mixing is considered for the ^{13}B ground state:

$$|\,^{13}\mathrm{B}(\mathrm{gs})\rangle=\alpha|(p_{3/2})^1_\pi\rangle+\beta|(p_{3/2})^1_\pi(p_{1/2})^{-2}_\nu(s_{1/2})^2_\nu\rangle.$$

Given this wave function, the width of the neutron peak is proportional to the spectroscopic factor $|\beta|^2$, and the value of $|\beta|^2$ can be evaluated by comparing the observed width Γ, with the single-particle width Γ_{sp} [47], where the latter is calculated to be 0.16 MeV using the channel radius of $1.5\times13^{1/3}$ fm. The ratio Γ/Γ_{sp}, which is equivalent to $|\beta|^2$, is then determined to be approximately 33%. This value is far different from the zero value expected from the naive picture of $N=8$ magicity, thereby indicating the influence of shell gap quenching.

In the above analysis the wave function of the initial state was simply taken as $|(1p_{3/2})^1_\pi(1p_{1/2})^{-1}_\nu(2s_{1/2})^2_\nu\rangle$. However, the wave function may contain other configurations such as that with $(1d_{5/2})^2_\nu$ instead of $(2s_{1/2})^2_\nu$. Also components associated with proton excitations may be mixed. Similarly the wave function of the final state is subject to further mixing of different components. In any of such cases, the theoretical estimate of the width should be effectively reduced. Hence the amplitude of the $2p$-$2h$ configurations should be even larger than the one obtained above.

The component relevant to $|\beta|^2$ represents a neutron configuration of two particles and two holes, where two valence neutrons in $(1p_{1/2})^2_\nu$ are excited to $(2s_{1/2})^2_\nu$. The large amplitude of this configuration in ^{13}B is not surprising but rather in good agreement with the conclusion of Sec. V A. The reduced energy gap between the $(1p_{1/2})_\nu$ and $(2s_{1/2})_\nu$ orbitals observed in the boron isotopes with $N=7$ and 9 should help to enhance the mixing of such a $2p$-$2h$ configuration for this boron isotope with $N=8$.

C. Reduction of the shell gap energy in ^{12}Be deduced from the log ft value of ^{14}Be β decay

The log ft value of the β transition from ^{14}Be to the 1^+ state in ^{14}B has a very small log ft value of 3.68. This is a clear evidence for an allowed transition, and can be used to elucidate the wave functions of the initial and final states.

The allowed β decay of ^{14}Be should be attributed to the transformation of a neutron in the p shell or sd shell into a proton with the same orbital angular momentum. In the case of ^{14}B, configurations with protons in the sd shell rarely exist at lower excited levels so that the β decay to the 1.28-MeV ^{14}B (1^+) state may be considered primarily due to the transformation of a p-shell neutron to a p-shell proton. On the other hand, the ground state of ^{14}Be may be assumed to have the major configuration of $|(sd)^2_\nu\rangle$ outside of the hypothetical ^{12}Be. In this case, the two outermost valence neutrons of ^{14}Be in the sd shell cannot participate in the β decay to the 1^+ state in ^{14}B. Hence, the transition of a p-shell neutron may only occur through the decay of the ^{12}Be core. This argument suggests a similarity between the ^{12}Be and ^{14}Be β decays as discussed by Timofeyuk and Descouvemont [48]. We thus compare the two β transitions, i.e., $^{12}\mathrm{Be}\,(0^+)\rightarrow{}^{12}\mathrm{B}\,(1^+)$ and $^{14}\mathrm{Be}\,(0^+)\rightarrow{}^{14}\mathrm{B}\,(1^+)$ since the initial and final states of these transitions are, respectively, nearly identical to each other after removing the two sd-shell neutrons from ^{14}Be and ^{14}B. We found that their log ft values are indeed very close to each other: The log ft value for the ^{12}Be branch is 3.83 [40], while it is 3.68 ± 0.05 for the ^{14}Be branch.

Nevertheless there remains a small difference between the two log ft values. This difference, -0.18 $(\Delta ft/ft=34\%)$, may be again associated with the reduced shell gap between the p and sd shells in ^{12}Be. As a matter of fact, Suzuki and Otsuka pointed out that the β decay of ^{12}Be to the ground state of ^{12}B is affected by such shell quenching [20]. In their analysis, the wave function of the ^{12}Be ground state required a mixture of $|0\rangle$ and $|(1p_{1/2})^{-2}_\nu(2s_{1/2})^2_\nu\rangle$ configurations. Since the latter configuration cannot participate in the β decay, the strength of the decay is accordingly reduced. By comparing the calculated ft value with the experimental value, the amplitude of the $|(1p_{1/2})^{-2}_\nu(2s_{1/2})^2_\nu\rangle$ configuration was found to be 66%. On the other hand the wave function of ^{14}Be involves two additional neutrons that are supposed to fill the valence orbitals of $(2s_{1/2})_\nu$ and/or $(1d_{5/2})_\nu$ [7,8]. Such occupancy of the outer neutrons should suppress the $2p$-$2h$ excitations. Hence the configuration of $|(1p_{1/2})^{-2}_\nu(2s_{1/2})^2_\nu(1d_{5/2})^2_\nu\rangle$, which is analogous to the $|(1p_{1/2})^{-2}_\nu(2s_{1/2})^2_\nu\rangle$ configuration for ^{12}Be, can hardly be mixed to the wave function of the ground state of ^{14}Be. Under these assumptions, the log ft value of the ^{14}Be decay

is identical to that of the hypothetical ^{12}Be decay that would occur, if the wave function of ^{12}Be only had the $|0\rangle$ configuration. In other words, the reduction of the *ft* value of ^{12}Be with respect to that of ^{14}Be can be ascribed to the mixing probability of the $|(p_{1/2})_\nu^{-2}(sd)_\nu^2\rangle$ configuration for ^{12}Be. The mixing probability thus obtained is 34%, which is compatible with the calculated value of 65% by Suzuki and Otsuka [20].

VI. SUMMARY

We studied the β decay of a neutron-rich isotope, ^{14}Be, by analyzing the β-γ, β-n, β-γ-n, and β-n-n coincidence data, and a revised decay scheme was established. The half-life and delayed neutron emission probabilities, P_{in} $(i=0,1,2)$ were determined to be 4.84 ± 0.10 ms, $P_{0n}<0.6\%$, $P_{1n}=94\pm5\%$, and $P_{2n}=6\pm5\%$, respectively. The β decay is dominated by a single branch followed by the emission of a 288-keV neutron. This branch has a very small log *ft* value of 3.68 ± 0.05 and leads to a hitherto unknown intruder 1^+ state of ^{14}B at the excitation energy of 1.28 ± 0.02 MeV with the width of 49 ± 2 keV.

The present results were analyzed in terms of a simple shell model. They all indicate a strong influence of the quenched shell gap between the *p* and *sd* orbitals as summarized below, revealing that significant phenomena due to the quenching occur not only for the $N=7$ isotones but also for the $N=8$ and $N=9$ isotones.

(1) The single-particle energy difference $\Delta\epsilon$ between the $1p_{1/2}$ and $2s_{1/2}$ orbitals was studied for $N=9$ isotones by incorporating the result of the excitation energy of the intruder 1^+ state of ^{14}B $(N=9)$. The behavior of $\Delta\epsilon$ with atomic number Z for $N=9$ isotones is found to be very similar to that of $N=7$ isotones, showing a significant reduction of $\Delta\epsilon$ for small Z isotopes.

(2) The observed decay width for the strong neutron peak allowed us to investigate the wave functions of the initial and final states. It was found that a large mixture ($\sim$33%) of the $2p$-$2h$ neutron excitation component, $(1p_{1/2})_\nu^{-2}(2s_{1/2})_\nu^2$, is necessary in the ground state wave function of ^{13}B $(N=8)$ to account for the *p*-wave neutron emission.

(3) The reason for a difference in log *ft* between ^{14}Be and ^{12}Be was investigated by comparing the wave functions of the ^{12}Be ground state and the ^{12}Be-like core for ^{14}Be, and it was found that the difference was attributed to a large mixture ($\sim$34%) of the $(1p_{1/2})_\nu^{-2}(2s_{1/2})_\nu^2$ component in the ^{12}Be $(N=8)$ ground state wave function and the suppression of such component due to Pauli blocking in the wave function of the core of ^{14}Be.

ACKNOWLEDGMENTS

The authors would like to thank the staff of the RIKEN Ring Cyclotron for the stable operation of the accelerator during the experiment and Professor M. Igashira and Dr. T. Shima for their help during the neutron detection efficiency measurement at RLNR. We are also indebted to Professor J.J. Kolata and Professor T. Otsuka for stimulating discussions. One of the authors (N.A.) gratefully acknowledges the financial support of the Japan Society for the Promotion of Science for Young Scientists.

[1] P.G. Hansen, A.S. Jensen, and B. Jonson, Annu. Rev. Nucl. Part. Sci. **45**, 591 (1995), and references therein.
[2] I. Tanihata, Prog. Part. Nucl. Phys. **35**, 505 (1995), and references therein.
[3] G. Audi and A.H. Wapstra, Nucl. Phys. **A565**, 66 (1993).
[4] I. Tanihata, T. Kobayashi, O. Yamakawa, S. Shimoura, K. Ekuni, K. Sugimoto, N. Takahashi, T. Shimoda, and H. Sato, Phys. Lett. B **206**, 592 (1988).
[5] T. Suzuki *et al.*, Nucl. Phys. **A658**, 313 (1999).
[6] M. Zahar *et al.*, Phys. Rev. C **48**, R1484 (1993).
[7] S. Takeuchi *et al.*, Phys. Lett. B **515**, 255 (2001).
[8] M. Labiche *et al.*, Phys. Rev. Lett. **86**, 600 (2001).
[9] Zhongzhou Ren, Gongou Xu, Baoqiu Chen, Zhongyu Ma, and W. Mittig, Phys. Lett. B **351**, 11 (1995).
[10] I. Talmi and I. Unna, Phys. Rev. Lett. **4**, 469 (1960).
[11] D.H. Wilkinson and D.E. Alburger, Phys. Rev. **113**, 563 (1959).
[12] H.G. Bohlen *et al.*, Z. Phys. A **344**, 381 (1993).
[13] T. Kobayashi, K. Yoshida, A. Ozawa, I. Tanihata, A. Korsheninnikov, E. Nikolski, and T. Nakamura, Nucl. Phys. **A616**, 223c (1997).
[14] S. Shimoura *et al.*, Nucl. Phys. **A616**, 208c (1997).
[15] H.G. Bohlen, W. von Oertzen, Th. Stolla, R. Kalpakchieva, B. Gebauer, M. Wilpert, Th. Wilpert, A.N. Ostrowski, S.M. Grimes, and T.N. Massey, Nucl. Phys. **A616**, 254c (1997).
[16] M. Zinser *et al.*, Nucl. Phys. **A619**, 151 (1997).
[17] S. Shimoura *et al.*, Nucl. Phys. **A630**, 387c (1998).
[18] J.A. Caggiano, D. Bazin, W. Benenson, B. Davids, B.M. Sherrill, M. Steiner, J. Yurkon, A.F. Zeller, and B. Blank, Phys. Rev. C **60**, 064322 (1999).
[19] Toshio Suzuki and Takaharu Otsuka, Phys. Rev. C **50**, R555 (1994).
[20] Toshio Suzuki and Takaharu Otsuka, Phys. Rev. C **56**, 847 (1997).
[21] A. Navin *et al.*, Phys. Rev. Lett. **85**, 266 (2000).
[22] H. Iwasaki *et al.*, Phys. Lett. B **481**, 7 (2000).
[23] H. Sagawa, T. Suzuki, H. Iwasaki, and M. Ishihara, Phys. Rev. C **63**, 034310 (2001).
[24] T. Kobayashi, Nucl. Phys. **A538**, 343c (1992).
[25] A.A. Korsheninnikov *et al.*, Phys. Rev. Lett. **78**, 2317 (1997).
[26] H. Iwasaki *et al.*, Phys. Lett. B **491**, 8 (2000).
[27] M. Langevin, C. Détraz, D. Guillemaud, F. Naulin, M. Epherre, R. Klapisch, S.K.T. Mark, M. de Saint Simon, C. Thibault, and F. Touchard, Nucl. Phys. **A366**, 449 (1981).
[28] M. Langevin, C. Détraz, M. Epherre, D. Guillemaud-Mueller, B. Jonson, and C. Thibault, Phys. Lett. **146B**, 176 (1984).
[29] I. Mukha *et al.*, Phys. Lett. B **367**, 65 (1996).
[30] M.J.G. Borge, L. Johannsen, B. Jonson, T. Nilsson, G. Nyman,

K. Riisager, O. Tengblad, and K. Wilhelmsen Rolander, Nucl. Phys. **A560**, 664 (1993).
[31] J.P. Dufour *et al.*, Phys. Lett. B **206**, 195 (1988).
[32] G. Audi and A.H. Wapstra, Nucl. Phys. **A565**, 1 (1993).
[33] U.C. Bergmann *et al.*, Nucl. Phys. **A658**, 129 (1999).
[34] M.D. Belbot *et al.*, Phys. Rev. C **51**, 2372 (1995).
[35] M.D. Belbot *et al.*, Phys. Rev. C **56**, 3038 (1997).
[36] N. Aoi *et al.*, Nucl. Phys. **A616**, 181c (1997).
[37] N. Aoi *et al.*, Z. Phys. A **358**, 253 (1997).
[38] T. Kubo, M. Ishihara, N. Inabe, H. Kumagai, I. Tanihata, K. Yoshida, T. Nakamura, H. Okuno, S. Shimoura, and K. Asahi, Nucl. Instrum. Methods Phys. Res. B **70**, 309 (1992).
[39] F. Ajzenberg-Selove, Nucl. Phys. **A523**, 1 (1991).
[40] F. Ajzenberg-Selove, Nucl. Phys. **A506**, 1 (1990).
[41] H. Ohm, W. Rudolph, and K.-L. Kratz, Nucl. Phys. **A274**, 45 (1976).
[42] H. Miyatake *et al.*, Phys. Rev. C (submitted).
[43] P.K. Joshi, H.C. Jain, A.S. Medhi, S. Chattopadhyay, S. Bhattacharya, and A. Goswami, Nucl. Instrum. Methods Phys. Res. A **399**, 51 (1997).
[44] G. Raimann *et al.*, Phys. Rev. C **53**, 453 (1996).
[45] K.W. Jones, W.R. Harris, M.T. McEllistrem, and D.E. Alburger, Phys. Rev. **186**, 978 (1969).
[46] H. Okuno *et al.*, Phys. Lett. B **354**, 41 (1995).
[47] A. Bohr and B.R. Motterson, *Nuclear Structure* (Benjamin, New York, 1969), Vol. 1, p. 441.
[48] N.K. Timofeyuk and P. Descouvemont, J. Phys. G **22**, L99 (1996).